We are IntechOpen,
the world's leading publisher of
Open Access books
Built by scientists, for scientists

5,800
Open access books available

142,000
International authors and editors

180M
Downloads

154
Countries delivered to

Our authors are among the

TOP 1%
most cited scientists

12.2%
Contributors from top 500 universities

BOOK CITATION INDEX
CLARIVATE ANALYTICS
INDEXED

WEB OF SCIENCE™

Selection of our books indexed in the Book Citation Index
in Web of Science™ Core Collection (BKCI)

Interested in publishing with us?
Contact book.department@intechopen.com

Numbers displayed above are based on latest data collected.
For more information visit www.intechopen.com

Chapter

Perovskite-Based Nanomaterials and Nanocomposites for Photocatalytic Decontamination of Water

Yousef Faraj and Ruzhen Xie

Abstract

The exploration of functional nanomaterials with superior catalytic activity for practical photocatalytic water decontamination is of significant importance. Perovskite-based nanomaterials, which demonstrate excellent photophysical and catalytic properties, are widely investigated as a class of adaptable materials for the photocatalytic degradation of environmental pollutants. This chapter introduces the recent progresses in using perovskite-based nanocomposites with particular emphasis on the applications for effective photocatalytic degradation of organic pollutants in wastewater. It starts by presenting the general principles and mechanisms governing photocatalytic degradation of organic pollutants in water by perovskite, along with the design criteria for perovskite-based nanocomposites. It then explains various strategies used to prepare perovskite-based nanocomposites with the aim of enhancing their photocatalytic activity. By the end of the chapter, the remaining challenges and perspectives for developing efficient perovskite-based photocatalysts with potential large-scale application are highlighted.

Keywords: perovskite, photocatalysis, water decontamination, reactive oxidation species, nanomaterials, nanocomposites

1. Introduction

The rapid growing population, urbanisation and industrial development are the major contributors of organic pollutants in water, which have a detrimental impact on the ecosystem, and cause serious problems to the living world and environment. In order to balance the ecosystem and mitigate the huge risk caused by the persistence organic substances, the removal of organic pollutants in wastewater is paramount.

Over the past two decades, solar photocatalysis has been of particular interest for the removal and degradation of organic pollutants in wastewater. In the photocatalytic water decontamination process, the production of electron-hole (e^--h^+) pairs via irradiation of the photocatalyst is the key step for the production of reactive oxidation species (ROS, i.e. hydroxyl radicals ($^\bullet OH$)), which is powerful oxidants and can

non-selectively attack organic matters, degrading them into smaller elements and finally mineralise them to H_2O and CO_2 [1]. Under light irradiation of a photocatalyst, photons with energy equal or greater than its band gap (E_g) are absorbed by the catalyst, resulting in the formation of an electron-hole pair. Then the photogenerated conduction band electron (e_{CB-}) and valence band hole (h_{VB+}) could undergo undesired recombination or participate in a series of reactions to produce highly Reactive Oxidation Species (ROS, i.e., hydroxyl radicals ($^•OH$)) that can mineralise any organic molecule in wastewater [2]. The necessity to find photocatalysts with unique photophysical properties that can be used efficiently in the photocatalysis process has been the driving force for the development of variety of material systems to achieve an efficient removal of organic pollutants. Different types of heterogeneous semiconductors, particularly titanium dioxide (TiO_2), ternary and other oxide systems, are the most widely studied materials for photocatalytic water decontamination. TiO_2, which is well known for its photocatalytic properties, widely used, low-cost n-type semiconductor with (E_g) of 3.2 eV, can be used for water decontamination and water splitting and building self-cleaning facades [3]. However, the major drawback of using TiO_2 in practical photocatalytic water decontamination is concerning two important aspects of its photocatalytic properties: (i) TiO_2 offers low photoconversion efficiency due to undesired recombination of electrons and holes [4] and (ii) its large band gap, which can be excited only by ultraviolet light (only 4% intensity of solar radiation) [5]. In addition, compared to other advanced oxidation processes (AOPs), such as Fenton based methods; UV/Oxidant methods and electrochemical oxidation methods, which can in-situ generate ROS during water treatment, the quantum yield of TiO_2 is low for photocatalytic ROS production, hindering its application in photocatalytic water decontamination [6]. Therefore, exploring novel photocatalysts that have unique photophysical properties, offer high photo-conversion efficiency and with superior photocatalytic activity in water decontamination application is of great importance.

Perovskite-based nanomaterial have attracted huge attentions as a promising photocatalysis nanomaterial for various environmental application due to their unique features such as high chemical and thermal stability; excellent electrical conductivity; and narrow band gap that can offer efficient use of solar energy, compared to other semiconductor photocatalysts. Perovskite-type oxides are complex metal oxides, with the general formula of ABO_3, the structure of which is shown in **Figure 1**. General structure of perovskite oxides represents a lattice that consists of larger A cations and are alkaline rare-earth metals, which are 12 fold coordinated by oxygen atoms, and small B cations that can be a divalent or trivalent transition, within oxygen octahedra. Their high stability under aggressive conditions is attributed to the existence of transition metals in their oxidation states [7, 8]. The structure of perovskites can easily be tuned by adjusting the category and proportion of their chemical compositions, which in turn inherit them diverse and unique physicochemical properties [9]. Perovskite oxides are capable of being activated by broad solar spectra to excite $e^−$-h^+ pairs and initiate the production of ROS, which facilitate organic pollutant oxidation and mainly comprise hydroxyl-radical ($^•OH$) and superoxide-anion radical ($O_2^{•−}$) [10]. However, pure perovskites suffer from low photocatalytic efficiency, which is due to small surface area of bulk material, insufficient solar energy consumption, rapid recombination and low redox potential of $e^−$-h^+ pairs, which are unfavorable for efficient generation of reactive species [11].

The performance of perovskites in photocatalysis process is generally influenced by their structure; composition; size and shape and synthesis process. Therefore, with the aim of enhancing their photocatalytic efficiency in the degradation of
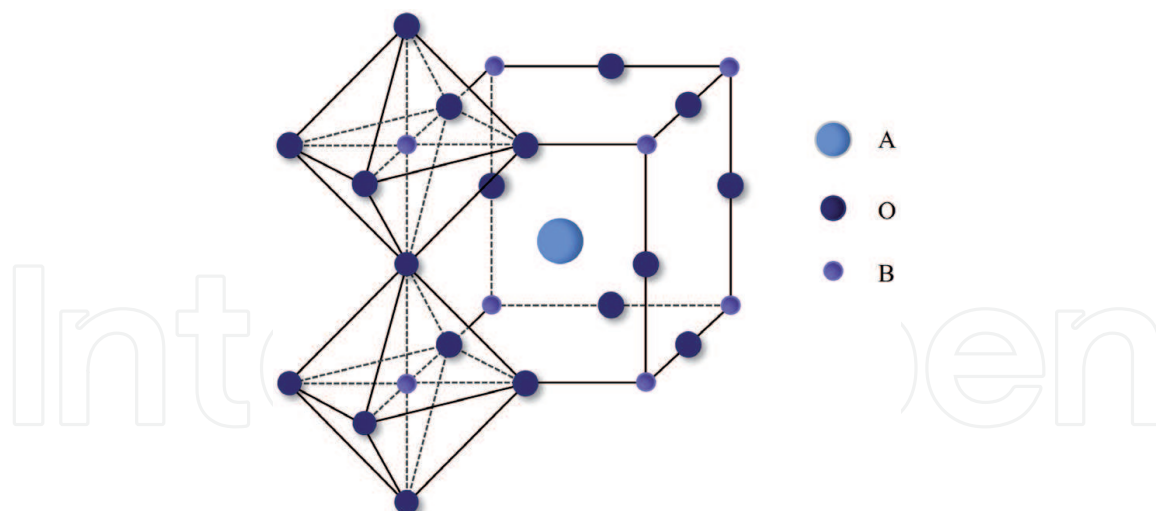
Figure 1.
ABO_3-type of perovskite structure (reprinted with permission from ref. [18]. Copyright © 2021, Elsevier).

organic pollutants, numerous studies have been carried, using various synthesis methods such as sol-gel method; hydrothermal; solvothermal; sono-chemical; microwave assisted method and co-precipitation method. In order to enhance the photocatalytic performance of perovskite, a number of strategies can be adopted, such as regulating perovskite composition through partial or full cationic substitution by certain dopant(s); rescaling its structure through downsizing or morphology alteration; hybrid modification through coating and coupling with other AOPs. It is worth pointing out that the strategy of coupling with other AOPs is beyond the scope of this chapter, therefore, no further reference will be made. The aforementioned strategies have been proven to improve perovskite's light absorption; create more active sites on the surface and inhibit e^--h^+ pairs recombination. By regulating perovskite composition through hetero-substitution of perovskite by hetero-valent or homo-valent cations in A and/or B site, the redox property of the perovskite is significantly improved and oxygen vacancies are increased, thereby promoting ROS generation [12]. Incorporating dopants into the lattice of perovskite, its inherent band gap can be reduced by shifting the top of its VB upward or CB downward, leading to an extended optical absorption improvement of its photocatalytic activity. Loading perovskite on substrates to obtain a hybrid nanostructure is an effective option for narrowing the band gap and optimisation of electronic structure to inhibit the recombination of e^--h^+ pairs. The coating strategy could address the majority of issues related to the efficient photocatalytic activity to some extent, as the coating strategy equip perovskite with an outstanding charge separation ability and strong oxidation ability. Rescaling structure and downsizing and controlling morphology of perovskites can be carried out to improve reactive sites and optimise optical absorption [13]. Smaller particle size can benefit from higher quantum efficiency due to larger accessible of reactive sites and more effective electron transfer paths. However, downsizing these particles to nanoscale increases the surface energy that prompts particles aggregation, hence elimination of the desired reactive sites and significant reduction of photocatalytic performance [14]. Controlled preparation of porous structure has been proven to equip perovskite with better optical absorption ability; increased reactive sites for photocatalytic reaction; as well as enhances the diffusion rate of organic pollutants. However, introducing pores to perovskite nanoparticles can make it physically fragile [15].

Despite intensive research studies that have been carried out on developing variety of nanoscale perovskite-based composites using different strategies, most of which with encouraging results, there is still much to be investigated. A comprehensive understanding of achieving an effective photocatalytic degradation of a wide range of organic pollutants using perovskites is highly crucial for unveiling the fundamental nature of perovskite photocatalysis for large-scale applications. In addition, to meet the requirements of designing efficient, stable and cost-effective perovskite-based composite photocatalyst with an outstanding use of solar energy for actual water remediation, a fundamental study of perovskite photocatalysis using different materials and various environmental pollutants is indispensable.

This chapter provides an overview of the state-of-the-art design and synthesis strategies for perovskite-based nanomaterials and nanocomposites for efficient water remediation. Initially the principles of photocatalysis process are described, with the emphasis on the mechanisms of photocatalytic water decontamination by perovskite and highlighting its inherent challenges. An evaluation of several strategies that have been used to develop perovskite-based nanocomposites for enhanced photocatalytic degradation of organic pollutants in water is presented. Finally, the remaining challenges and perspectives for developing novel perovskite-based photocatalysts with potential large-scale application are elucidated.

2. General principles of perovskite photocatalysis process

In photocatalytic process, perovskite uses photon as a source of energy to initiate chemical reaction. As the photocatalyst is irradiated by light with energy equal or larger than the perovskite band gap, the electrons are excited from the valance band (VB) to the conduction band (CB), as a result photoreactive species such as e^- and h^+ are created, which can be transferred to the surface of perovskite [16]. The factors affecting the photocatalytic activity of perovskite as a catalyst are namely, the excitement of the electron, separation of the electron and hole and photo-oxidation reduction reaction taking place at the surface of the catalyst [17].

2.1 Mechanisms of photocatalytic degradation of pollutants in water by perovskite

The mechanisms of photocatalytic degradation of organic pollutants consists of several steps: (1) under light irradiation perovskite absorbs photon with an appropriate energy to form photoreactive species like e^- and h^+; (2) interfacial charge transfer; (3) reduction and oxidation process to form Reactive Oxidation Species; (4) degradation of organic pollutants; and (5) desorption of pollutants/intermediates from the surface of the perovskite. The reaction mechanisms of photocatalytic degradation of pollutants in water are demonstrated by Eqs. (1)–(5) [18].

$$\text{Perovskite} + \text{Light} \rightarrow \text{Perovskite}\left(e_{cb}^- + h_{vb}^+\right) \tag{1}$$

$$e_{cb}^- + O_2 \rightarrow O_2^{\cdot -} \tag{2}$$

$$h_{vb}^{+} + H_2O \,/\, OH^{-} \rightarrow \cdot OH \tag{3}$$

$$O_2^{-} \,/\, \cdot OH + \text{Organic Pollutants} \rightarrow \text{Intermediates}, CO_2, H_2O\ldots \tag{4}$$

$$h_{vb}^{+} + \text{Organic Pollutants} \rightarrow \text{Intermediates}, CO_2, H_2O\ldots \tag{5}$$
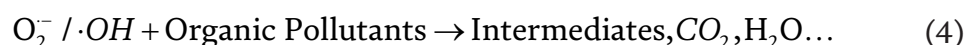
Under light irradiation of perovskite, when the energy of photon is equal or larger than the perovskite band gap energy, the electrons are excited from the valence band (VB) of perovskite to the conduction band (CB), as a result of which the photoactive species (e^- and h^+) are formed. The photoexcited electrons would either reunite with holes or transfer to the surface of the perovskite, which can react with O_2 to form superoxide anion radical ($O_2^{\bullet-}$), while the photogenerated holes react with water to form hydroxyl radical ($^{\bullet}OH$) at the surface of the catalyst [19]. The schematic representation of the degradation mechanism is illustrated in **Figure 2**. In this process, $\cdot OH$ acts as a powerful oxidising agent that attacks the organic molecules non-selectively.

Figure 3 shows the bandgap values, CB and VB positions, of several perovskite photocatalysts. It is apparent that pristine perovskites have the valance band potential energy (E_{vb}) higher than the $^{\bullet}OH/OH^-$ redox potential, which allows for the generation of $\cdot OH$ during the photocatalysis process. Nonetheless, the higher position of CB compared to that of the redox potential of $O_2/O_2^{\bullet-}$, hinders the formation of $O_2^{\bullet-}$ during the photocatalytic degradation process. Therefore, during the ROS production on perovskite, in order for the electrons to react with O_2 and form $O_2^{\bullet-}$, the conduction band potential (E_{cb}) of perovskite should be more negative than the standard redox potential of $O_2/O_2^{\bullet-}$ (-0.33 eV vs. NHE). On the other hand, the valance band potential energy (E_{vb}) of perovskite should be higher than standard redox potential of $^{\bullet}OH/OH^-$ ($+1.99$ eV vs. NHE). In such case, the OH^- can be oxidised by the photogenerated holes and form $^{\bullet}OH$, which can attack pollutants to convert them to nontoxic forms or completely degrade them to CO_2 and H_2O [20].
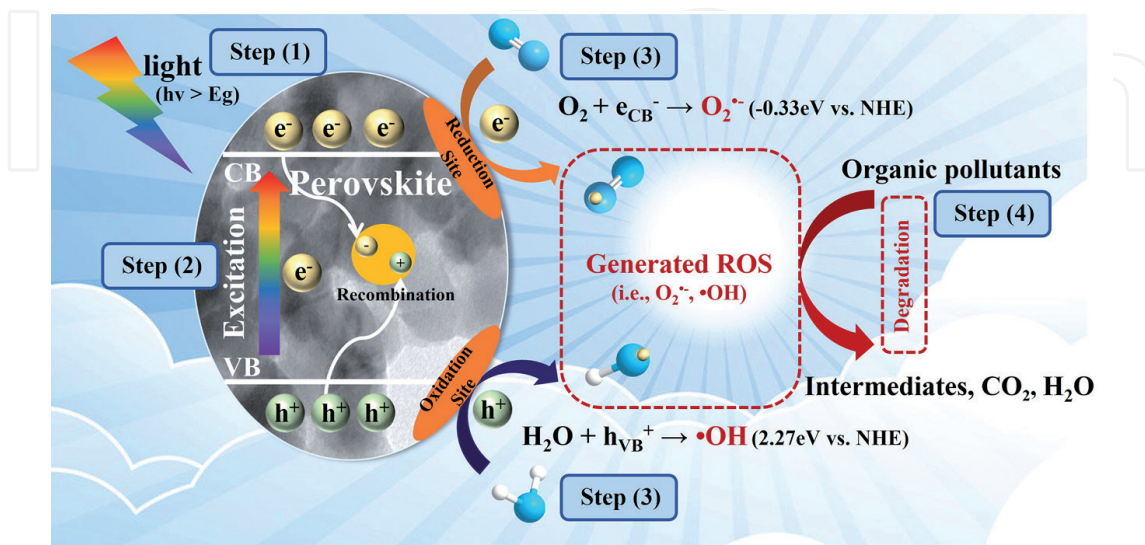
Figure 2.
Schematic representation of photocatalytic degradation of organic pollutants and ROS production by perovskite (reprinted with permission from ref. [18]. Copyright © 2021, Elsevier).
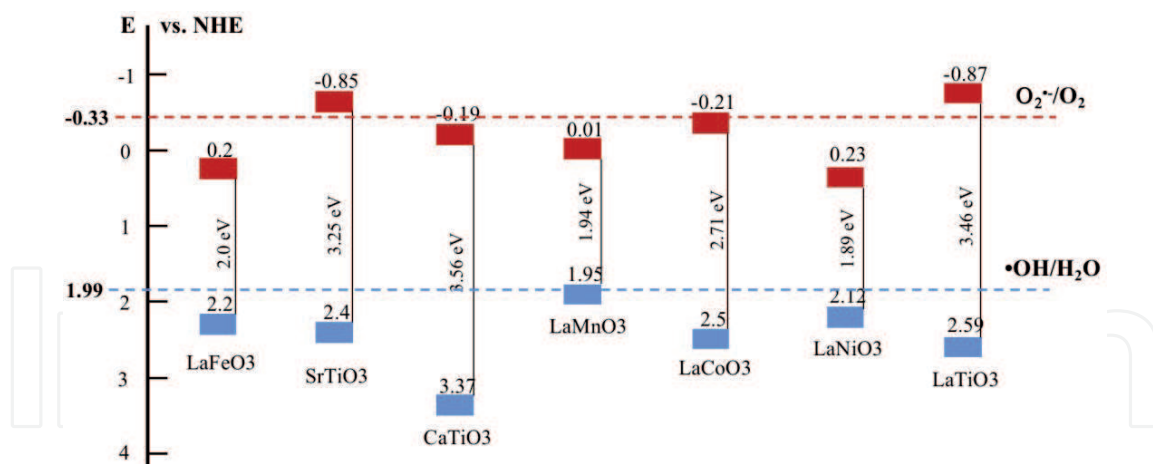
Figure 3.
Band gap values of several perovskite photocatalysts (Adapted with permission from ref. [18]. Copyright © 2021, Elsevier).

2.2 Perovskite design criteria for photocatalytic degradation of organic pollutants

The main criteria for a perovskite photocatalyst to be used in the degradation of organic pollutants in water are high capability of being activated by photons; efficiently extracting electrons for photocatalytic reaction; chemically stable; nontoxic; and cost effective. The absorption of photons the following charge generation is dependent on the physiochemical property of the perovskite and recombination.

The efficient use of solar energy still remains a great challenge. An ideal perovskite photocatalyst should have an enhanced and broaden light absorption, and capture a wide spectrum, from ultraviolet to visible light and even the near-infrared region. Therefore, it is necessary to adopt strategies that lead to optimisation of light harvesting, improving e^--h^+ separation, and generating sufficient active sites on the perovskite surface for photocatalytic reaction to take place A number of strategies have been reported in the literature, such as cationic substitution, nanostructure perovskite, coating and combined perovskite-based photocatalyst systems, in which perovskite is coupled with other AOP systems. The main aim of these state-of-the-art strategies is to enhance efficient light utilisation, improve charge separation and create richer active sites on the surface of the perovskite. Narrowing band gap is usually the option for the increased light harvesting by capturing more excited photons form a wide spectrum, and consequently enhancing photocatalytic activity [21].

Once the photogenerated charges are generated and successfully migrated to the surface of perovskite, where photocatalytic reactions take place, they can still undergo surface recombination or be trapped by undesirable reactants. In the photocatalytic process the e^--h^+ pairs are generated within several femtoseconds (fs) and undergo recombination within picoseconds (ps) to nanoseconds (ns), as depicted in **Figure 4**. However, the time span from the bulk to reactive sites is usually hundreds of ps, and the reaction time between the carriers and the adsorbed reactants requires nanoseconds (ns) to microseconds (μs) [22]. The lifetime of the photogenerated charges of some perovskites have been reported as BTO: 3.25 ns, STO: 2.06 ns, LFO: 3 ns and LMO: 2 ns, knowing that the reaction time to form $O_2^{\bullet-}$ is several nanoseconds [22]. This implies that the relatively short lifetime of the carriers on perovskite limits their application in photocatalytic degradation of organic pollutants.
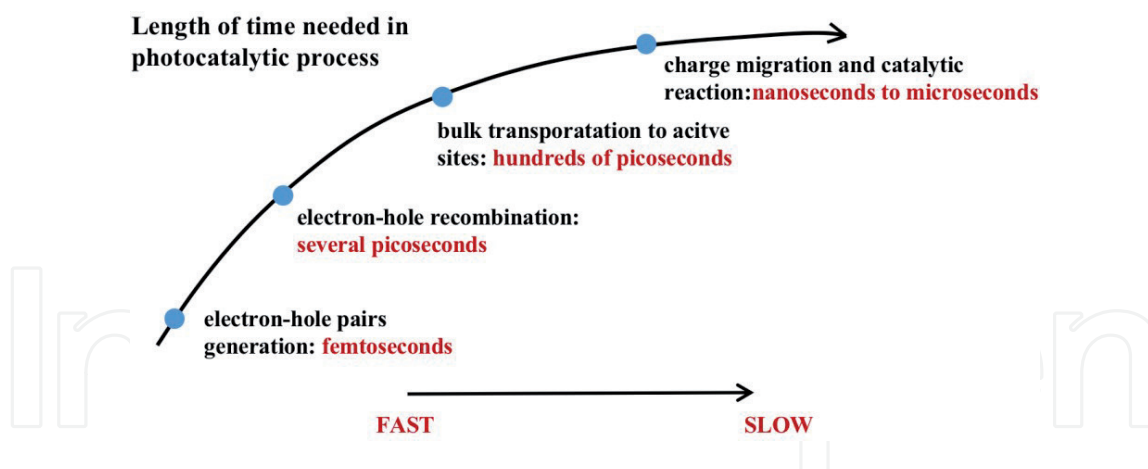
Figure 4.
Different length of time required in photocatalytic process.

In general, photocatalytic degradation takes place on the surface of the perovskite photocatalyst. Therefore, to improve photocatalytic degradation efficiency, a good adsorption of organic pollutants on the surface of perovskite is necessary. Undoubtedly, larger surface area is required to provide higher adsorption capacity towards organic pollutants and richer active sites for photocatalytic degradation reaction. A shorter diffusion pathway of charge carriers is also expected, as it reduces chance of e^--h^+ recombination.

3. Modification strategies for enhancement of perovskite photocatalytic activity

Although pure perovskites are potentially better than other oxide photocatalysts, their weak photocatalytic activity hinders their employment in industrial application. Undoubtedly, this is due to their inherent photocatalytic issues such as: (i) small surface area; (ii) insufficient solar energy utilisation; (iii) fast recombination rate of e^--h^+. To improve carriers' utilisation, a number of modification strategies have been reported, through which nanomaterials and nanocomposite materials are developed with significantly high photocatalytic performance. Some of these strategies are described in detail in the following sections.

3.1 Partial or full cationic substitution

Poor photocatalytic degradation of pristine perovskite under visible light (>400 nm) is mainly attributed to the wide band gap [23], which hiders its potential application in the degradation of organic pollutants. The photocatalytic properties of perovskite can be modified by partial or full cationic sites substitution. The partial or full cationic substitution can narrow the band gap and inhibit the recombination of e^--h^+, which leads to a significant enhancement of their photocatalytic activity. The substitution can be made in A-site, B-site or both sites, the detailed description of each type of substitution is provided in the following sections. It is worth mentioning that a number of factors can affect the substitution such as the types and concentration of dopant atoms, the substitution sites and so on. It is worth mentioning that the substitution of A-site, B-site or both sites in perovskite induces lattice defect and

adjusts its optical and redox properties, thereby enhancing the photocatalytic degra-dation of organic pollutants [24].

However, choosing the right substitute is very important in maintaining the perovskite crystal structure. The stability of A-site substituted perovskite with cubic structure can be defined through Goldschmidt's tolerance factor *t* as shown in Eq. (6) [25]:

$$t = \frac{r_A + r_O}{\sqrt{2}\left(r_B + r_O\right)} \tag{6}$$

Where r_A, r_B and r_O are ionic radii of A-site, B-site and oxygen ion, respectively.

Since the cubic structure of perovskite is stabilised at $0.76 < t < 1.13$, then almost 90% of the natural metal elements of the Periodic Table can be incorporated into the perovskite lattice. Thus, various common metal elements, as shown in **Figure 5**, can be used to substitute A or B cationic sites in perovskite to narrow the band gap and enhance its photocatalytic activity [26, 27].

The performance of various substituted perovskites with different substitution type and dopants used in substituting A-site, B-sites and both sites in the degradation of organic pollutants is highlighted in **Table 1**.

3.1.1 A site substituted perovskite

Substitution of a metal in A-site can have a direct impact on the structure and stability of perovskite. For example, partial substitution of A′ metal on A-site, having a modified perovskite with the general formula of $A_{1-x}A_x'BO_3$, can cause the creation of vacancies in the lattice [28]. Partial substitution of A-site in perovskite is also capable of modifying the valence state of cations in B-site, leading to a better redox property and a higher photocatalytic activity. For example, substitution of La^{3+} by K^+ in A-site of $LaCoO_3$ results in modification of Co^{3+} into Co^{4+} in $La_{1-x}K_xCoO_3$ [29]. The concentration of dopants or substitutes in partial substitution of A-site is an impor-tant factor that can affect the crystal size, band gap and oxygen vacancy content. By incorporating different concentrations of La^{3+} into the lattice sites of the $SrTiO_3(STO)$

Figure 5.
Metal elements as substitutes in the ABO_3 perovskite lattice [26].

Pure perovskite	Type	Dopant	Target pollutant	Performance of substituted perovskite	Ref.
LaFeO$_3$	A-site	Eu/Gd/ Dy/Nd	Safranine-O (15 mg/L)	7 times higher degradation rate than that by pure LFO	[99]
LaFeO$_3$	A-site	Ti	4-Cl-phenol (25 mg/L)	Complete removal and highest mineralization rate	[8]
LaFeO$_3$	A-site	Li	Methylene blue (78.54 mg/L)	45.7% removal compared to 35.1% by pure LFO	[32]
LaFeO$_3$	A-site	Ca	Methylene blue (10 mg/L)	77.5% removal compared to 48.9% by pure LFO	[33]
LaFeO$_3$	A-site	Bi	2,4-dichlorophenol (10 mg/L)	61% removal compared to 28% by pure PLFO	[100]
LaTiO$_3$	A-site	Ba/Sr/Ca	Congo red (100 mg/L)	75.33% degradation compared to 50.8% by pure LTO	[30]
SrTiO$_3$	A-site	Eu	RhB (5 mg/L)	95% removal, 2.6 times higher than that by pure STO	[105]
SrFeO$_3$	A-site	Pr/Sm	RhB (5 mg/L)	86% degradation efficiency compared to 43% by pure SFO	[103]
LaFeO$_3$	B-site	Mn	Methyl orange (100 mg/L)	96.4% removal higher than that by pure LFO	[45]
LaFeO$_3$	B-site	Cu	Acidpink 3B (10 mg/L)	97.4% removal compared to 62.2% by pure LFO	[101]
SrTiO$_3$	B-site	V/Mo	Methylene blue (10 mg/L)	91.5% removal compared to 59.9% by pure STO	[46]
SrTiO$_3$	B-site	Bi/Cu	Dibutyl phthalate (10 mg/L)	Higher degradation efficiency compared to pure STO	[48]
SrTiO$_3$	B-site	V	Methylene blue (10 mg/L)	Higher degradation efficiency compared to pure STO	[41]
SrTiO$_3$	A- & B-sites	La, Fe	Methyl Orange (10 mg/L)	Removal 19 times higher than that by pure STO	[104]
SrTiO$_3$	A- & B-sites	La, Cr	RhB (5 mg/L)	Removal 6 times higher than that by pure STO	[102]

Table 1.
Performance of various substituted perovskites.

host structure, different crystal defects and impurity energy levels can be formed on La-STO, resulting in different band gaps. Higher concentration of La^{3+} doping results in the decreased particle size of La-STO. However, an excessive concentration of the doping element can act as recombination center for photoinduced pairs and lead to a declined photocatalytic activity.

Various alkaline-earth metallic ions (i.e., Ba, Ca, and Sr) and rare-earth metals (i.e., La, Ce, Eu and Nd) can be used to substitute A-site of perovskite, which can result in narrowing band gap, generation of large amounts of oxygen vacancies and

improved photocatalytic efficiency for the degradation of organic pollutants under visible light [30, 31]. Partially substituting La^{3+} with Li^+ via sol-gel method yields a modified perovskite powder ($La_{0.97}Li_{0.03}FeO_3$) with improved photocatalytic degradation towards methyl blue. Since Li^+ has lower charge than La^{3+}, the charge neutrality is maintained by forming oxygen defects on the surface of $La_{0.97}Li_{0.03}FeO_3$, which leads to improved photocatalytic activity [32]. Incorporating Ti into A-site of pure $LaFeO_3$(LFO) via solid-solid diffusion results in reduced band gap and enhanced photocatalytic activity of the modified perovskite ($La_{1-x}Ti_xFeO_3$) for the degradation of 4-chlorophenol without iron leaching. Substituting La^{3+} in pure $LaFeO_3$ (LFO) with an appropriate amount of Ca^{2+} in LFO can be a feasible strategy to improve photocatalytic degradation of methylene blue under visible light [33]. Due to smaller radius of Ca^{2+} (0.134 nm) compared with La^{3+} (0.136 nm), the substitution of Ca^{2+} affects the crystalline size and the amount of charge-compensating oxygen vacancies in $La_{1-x}Ca_xFeO_3$. The charge-compensating oxygen vacancies can act as Lewis acid sites to capture electrons, and also narrow the band gap, which increases light harvesting by capturing more excited photons [34].

3.1.2 B site substituted perovskite

The B-site element in perovskite plays a more important role than the A-site element in photocatalytic reaction, as the redox reactions generally take place at the B-site element, and it can serve as a photocatalytic active center for most of the perovskites [35]. Doping B-site with divalent or trivalent cations induces the creation of oxygen defects, leading to a relaxation structure of $AB_{1-x}B'_xO_3$ with enhanced photocatalytic degradation activity [36]. Substituting Mn into the lattice of $SrTiO_3$ (STO) via hydrothermal method yields a visible-light-responsive photocatalyst, Mn-doped STO (MSTO), having a narrower band gap and higher photocatalytic degradation efficiency towards antibiotic tetracycline [37]. Mn^{4+} species (0.067 nm) could partially substitute Ti^{4+} (0.068 nm) into STO lattice and act as impurity energy band to narrow the band gap of STO and suppress the e^--h^+ recombination, hence creating sufficient time for photogenerated holes to oxidize water and form $\cdot OH$ for efficient photocatalytic degradation of tetracycline. Furthermore, substituting the B-site of perovskite by Cr yields advanced photocatalytic materials, in which the Cr^{3+} donor levels act as intermediate states for photon transition, allowing easier excitation of electrons and holes under visible light [38]. However, the presence of hexavalent Cr(VI) can hinder the photocatalytic activity of the catalyst [39]. Substitution of Fe^{3+} (0.064 nm) by a larger ionic radius Cu^{2+} (0.072 nm) in B-site of LFO results in lattice distortion, induced oxygen vacancies generation and suppressed the growth of large crystallite. This implies that a larger specific area with more accessible active sites is available for improved photocatalytic activity.

Substitution of the B-site perovskite with multiple valance cations results in coexistence of various cation states (i.e., Mn^{3+}/Mn^{4+}, Cu^+/Cu^{2+} and V^{3+}/V^{5+}) in perovskites [40, 41]. The presence of high valence ions can trap the photo-generated electrons in the CB, thereby the e^--h^+ pairs recombination is suppressed. While the low valence ions may supply electrons to the absorbed O_2 on the surface of the catalyst, enhancing interfacial electron transfer and increasing the photocatalytic degradation of organic pollutants in water [42]. Substitution of B-site in LFO lattice by Cu results in $LaFe_{0.85}Cu_{0.15}O_3$ with larger specific area and reduced band gap compared to LFO [43]. Under light irradiation of $LaFe_{0.85}Cu_{0.15}O_3$, the reduction of Fe^{3+} and Cu^{2+} can be accelerated and leads to the generation of Fe^{2+} and Cu^+. The presence

of the redox couples of Fe^{2+}/Fe^{3+} and Cu^+/Cu^{2+} plays an important role in the creation of ·OH and other ROS, which degrade organic pollutants [44]. Doping Mn in LFO via stearic acid solution combustion method results in $LaFe_{0.5}Mn_{0.5}O_{3-\delta}$ with higher photocatalytic efficiency for methyl orange degradation under sunlight, owing to the coexistence of variable valences of Mn ions such as $Mn^{2+}/Mn^{3+}/Mn^{4+}$ [45]. The lower valence Mn^{2+} and Mn^{3+} provide electrons and reduce O_2 to generate more $O_2^{\bullet-}$, while the stable Mn^{4+} traps electrons and suppresses electron-hole recombination.

Substitution of the B-site perovskite by multiple cations can create a synergistic effect, leading to an enhanced perovskite photocatalytic activity and improved stability. The photocatalytic degradation of methylene blue can be enhanced by co-doping of Mo and V in STO [46]. The Mo and V cations incorporated into the B-site of perovskite can create impurity defects, leading to reduced band gap value and enhanced visible light utilisation. The photocatalytic activity of multiple cations doped perovskite, such as Bi and Cu doped STO, is much higher than a single cation doped perovskite [47]. The highest degradation of dibutyl phthalate can be achieved by STO co-doped with both Bi and Cu in B-stie [48].

3.1.3 A and B sites substituted perovskite

Simultaneous substitution of A- and B-sites is a feasible strategy and can increase the photocatalytic efficiency of perovskite. Since the perovskite lattice offers a great flexibility in atomic arrangement, reasonable regulation of both A- and B-sites in perovskite can produce high performance $A_{1-x}A'_xB_{1-x}B'_xO_{3-\delta}$ with improved electronic and photocatalytic properties. In general, the substitution of A-site cation leads to the generation of oxygen vacancies, whereas the substitution of B-site mainly tunes the band structure and brings about the formation of redox couples.

Simultaneous substitution of A- and B-sites of STO by La and Ni, respectively, leads to a larger surface area and new defect bands for highly efficient photocatalytic decomposition of MB compared to La or Ni mono-doped STO [49]. The substitution of both A- and B-sties of $LaCoO_3$ leads to the creation of a modified perovskite photocatalyst $La_{0.5}Ba_{0.5}Co_xMn_{1-x}O_{3-\delta}$. The partial substitution of La^{3+} by Ba^{2+} in A-site results in improved catalytic activity and structural stability. While the substitution of B-site by Mn can further enhance the photocatalytic reactivity as a result of the formation of Co—O—Mn bond, offering accelerated electron transfer between the redox couples of Co^{2+}/Co^{3+} and Mn^{3+}/Mn^{4+}. Doping perovskites with non-metal ions such as C, P, S, N, F and B is also a feasible strategy to narrow the band gap, which is necessary in enhancing photocatalytic activity of perovskite for water decontamination [50, 51].

3.2 Perovskite nanocomposites via coating strategy

Pristine perovskites show relatively weak photogenerated charge separation rate and low surface area. In addition, photo-generated e^--h^+ pairs in some narrow-band gap perovskites tend to recombine, which results in considerable energy loss. Therefore, nanoengineered perovskite particles may address the above issues and provide high surface area, full utilisation of solar energy, efficient light absorption and effective e^--h^+ separation. However, Perovskite nanoparticles can undergo agglomeration during synthesis, which endows inferior photocatalytic performance. In order to address the particle agglomeration issue and achieve efficient charge separation and good dispersion, coating perovskites on various supports has been proven to be a feasible strategy. In addition, by composing suitable cocatalysts, the

photocatalytic reaction can be accelerated through lowering the activation energy. Loading perovskite on supports provides efficient charge migration and better pollutants adsorption capacity, which is crucial for improving photocatalytic activity. The loading amount can easily be tuned by simply changing the coating times and the concentration of the coating solutions. Given an appropriate support loading, abundant active sites are available for charge-transfer reactions, also the photogenerated carriers can be trapped on the supports to suppress e^--h^+ recombination. Perovskites can be coated on various supports such as carbon, silica, graphene, zeolites, semiconductor cocatalysts and so on.

3.2.1 Nanocomposite of perovskite and carbon-based materials

Carbonaceous materials have been widely studied and used in many applications, due to their outstanding characteristics such as large surface area, good electronic properties and excellent corrosion resistance. Loading perovskites on Carbon-derived materials can enhance photocatalytic degradation of organic pollutants, as they usually act as electron scavengers, owing to their large electron storage capacity. Composites of perovskite with carbon-based materials such as graphene oxide (GO) and its derivatives (graphitic carbon nitride and carbon aerogel) provide enhanced adsorption capacity towards organic pollutants, along with formed junctions, which hinders the e^--h^+ recombination.

Perovskite/GO composites have been proven to provide excellent photocatalytic activity in the degradation of organic pollutants. It is worth mentioning that the bandgap of the perovskite/GO composites can easily be tuned by incorporating perovskite with different proportions of GO. $LaMnO_3$/graphene composite has been reported to have a superior visible-light responsive photocatalytic activity in the degradation of diamine green B [52]. The photo-generated electrons migrate from $LaMnO_3$ (LMO) to GO across the heterojunction and temporarily stored on the surface of GO, suppressing electrons and holes recombination. The LMO particles are highly dispersed on the surface of GO, allowing them full exposure to light irradiation and high photon absorption, which improves the photocatalytic quantum efficiency. Compared to pure LMO, the decreased band gap in LMO/GO results in an obvious red shift of 30–40 nm in the light absorption edge, which enhances its photocatalytic activity. GO and STO composite can be prepared by hydrothermal method for efficient degradation of organic pollutants [53]. During heat treatment, GO is decomposed, and followed by the diffusion and dissolution of carbon species, which can penetrate into STO lattice and substitute its interlayer O^{2-} sites, thereby introducing C 2p state within the band gap. Under light irradiation, the photoexcited electrons on STO can easily be transferred to carbon and promote charge separation, resulting in an increased amount of reactive oxidation species for efficient degradation of organic pollutants.

Graphitic carbon nitride (g-C_3N_4), which is one of the most promising visible-light-driven photocatalysts, is another non-metallic material with unique layered structure and narrow band gap of 2.7–2.8 eV. However, the application of pristine g-C_3N_4 is limited by the rapid recombination of photoinduced e^--h^+. This issue can be addressed by adopting strategies to couple g-C_3N_4 with perovskites, thereby developing catalysts with high photocatalytic properties. $LaNiO_3$/g-C_3N_4 Z-scheme nanosheet has been prepared, in which 30 wt.% $LaNiO_3$ loading provides intimate attachment of LNO on the surface of g-C_3N_4, leading to the formation of abundant heterojunctions at the interface that are required for the spatial isolation of photogenerated charge carriers. Under light irradiation of

the $LaNiO_3$/g-C_3N_4 hybrid, the accumulated electrons with stronger reducibility can reduce O_2 to yield $O_2^{\bullet-}$. As a result, the $LaNiO_3$/g-C_3N_4 composite exhibits remarkable photocatalytic activity in the degradation of tetracycline, which is 3.8 times and 3.9 times faster than those of pristine g-C_3N_4 and $LaNiO_3$, respectively. Loading p-type semiconductor LFO with n-type g-C_3N_4 nanosheets results in a hybrid p-n heterostructure photocatalyst (LFO/g-C_3N_4) that exhibits superior photocatalytic activity, compared to pristine g-C_3N_4 and LFO, in the degradation of Brilliant Blue [54].

3.2.2 Nanocomposite of perovskite and metal oxide

Metal oxide is regarded as a promising supporting material for perovskites to achieve higher photocatalytic activity in degradation of organic pollutants. By forming heterojunctions between metal oxides and perovskite, the metal oxides act as co-catalysts, serve as charge collectors to facilitate charge separation and efficiently extend the lifetime of the charge carriers. Metal oxides such as TiO_2, ZnO, and CeO_2 are abundant in nature and have been widely used as alternative catalysts to precious metals in various chemical reactions [55].

A number of metal oxides, such as ZnO, CeO_2, Al_2O_3, CuO, MnO_2 and WO_3 have been used in perovskite coating [56–59]. It can be argued that the most widely used metal oxide to couple with perovskites is TiO_2 [60–62]. The STO/TiO_2 nanofiber has been synthesised via hydrothermal method, using TiO_2 as both template and reactant [63]. Under UV light irradiation, the photogenerated electrons are transferred from STO to TiO_2 due to their close contact, thus improving the interfacial charge migration to the adsorbed substance. The electrons react with dissolved O_2 to form $O_2^{\bullet-}$ and subsequently protonated to strong oxidizing agents like H_2O_2, $HO_2^{\bullet}$ and ·OH. Reportedly, the incorporation of TiO_2 into STO can prolong the lifetime of photoinduced charge carriers. It has been demonstrated that the combination of TiO_2 and $LaNiO_3$ can significantly enhance the photocatalytic activity of the modified perovskite in degradation of methyl orange and antibiotic ciprofloxacin under visible light. The $LaNiO_3$/TiO_2 step-scheme (S-scheme) can be synthesised via a facial sol-gel method as shown in **Figure 6**, in which the S-scheme heterojunction is formed between the n-type TiO_2 and p-type $LaNiO_3$ due to the potential energy difference of VB in TiO_2 and CB in $LaNiO_3$. Exploiting the electric field and band edge bending, the electrons can spontaneously be transferred from TiO_2 CB to $LaNiO_3$ across the interfacial region until they reach similar Fermi level. O_2 is reduced to $O_2^{\bullet-}$ by the accumulative electrons in the CB of $LaNiO_3$ with more negative potential, while the remaining holes in the VB of TiO_2 oxidises H_2O to ·OH, thereby the photocatalytic activity of the coupled TiO_2 and $LaNiO_3$ is significantly promoted. In another study, STO is coated on WO_3, in which an efficient Z-scheme heterojunction is obtained [64]. Under visible light irradiation of the modified STO, the electrons in the CB of WO_3 tend to recombine with the holes in STO, thus the electrons in the CB of STO and holes in the VB of WO_3 can separate and form reactive oxidation species for efficient degradation of pollutants in water.

3.2.3 Nanocomposite of perovskite and silica-based material

Perovskites can be coated on silica-based material for efficient charge separation and enhancement of absorption capacity, thus increasing their potential application in photocatalytic degradation of pollutants in water. Coating perovskites on porous
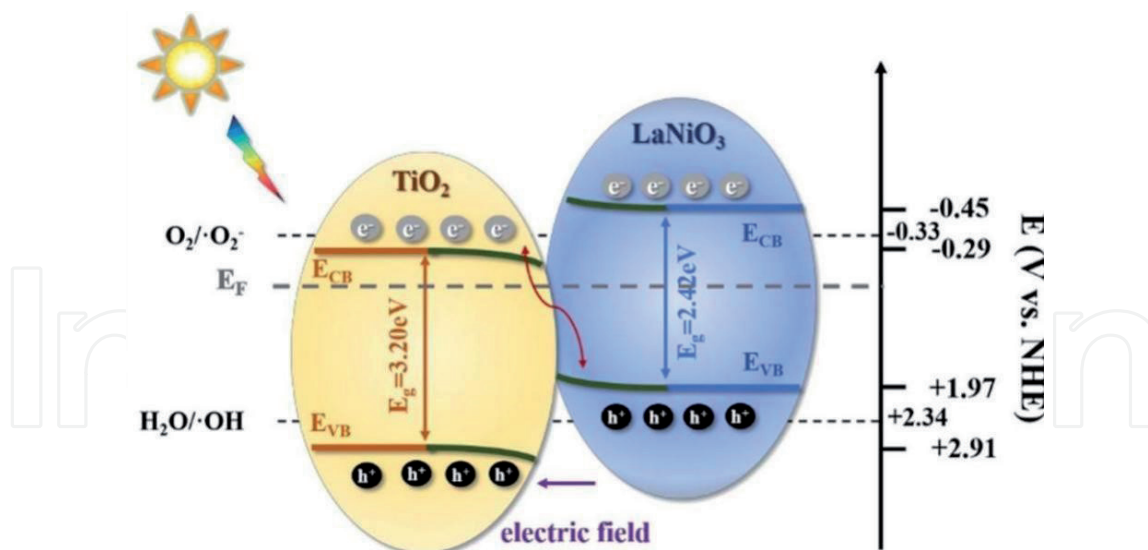
Figure 6.
Schematic representation of LaNiO₃ and TiO₂ nanocomposite [62].

silica can also provide easier transport of large organic molecules and the availability of more active sites, which results in efficient photo-Fenton catalytic degradation [65]. Various clay minerals such as montmorillonite, bentonite, kaolinite, illite and zeolite have been used as supporting materials for perovskites, which provide significant adsorptive capacity for the removal of toxic organic pollutants in aqueous solutions [66]. The porous silica support play two key roles in the degradation process, enhancement of the adsorption capacity via hydrogen bonds formed between the support and organic pollutants, and transportation of adsorbed substance to active sites.

Montmorillonite (MMT), which is one of the most abundant clay minerals and possesses ample —OH groups on the surface, has been used as a support for LFO to form a nanocomposite of LFO/MMT for effective removal of Rhodamine B in water. The presence of —OH groups on the surface of MMT allows LFO to be uniformly distributed on the surface of montmorillonite via Si—O—Fe bonds, which results in LFO/MMT with higher surface area and enhanced photocatalytic activity. LFO/MMT can effectively remove Rhodamine B (RhB) via synergistic effect of adsorption and photocatalytic degradation [67]. Different LFO/silica composites have been prepared and studied using several mesoporous silica materials (SBA-15, SBA-16 and siliceous mesostructured cellular foams (MCF)), along with nano-sized silica powder as supports for photocatalytic degradation of RhB [68]. Compared with other nanocomposites and pure LFO, LFO/MCF demonstrates the highest photocatalytic activity towards RhB. The superior photocatalytic activity of LFO/MCF can be attributed to the randomly distributed pores and short pore length of MCF, which allows easier and faster transportation of RhB to the active sites within the pores of LFO/MCF.

Zeolite, which is a crystalline aluminosilicate material, is another widely used supporting material for perovskites to enhance the photocatalytic degradation of organic pollutants. Using zeolite for loading perovskite can provide an effective nanocomposite with high photocatalytic activity, as its cages and pores enable easier and faster mass transfer of adsorbed substance, it provides abundant active sites for photocatalytic degradation of pollutants and can control the charge transfer process to reduce the e⁻-h⁺ recombination [69]. To optimise physicochemical properties of zeolite, such as adsorption capacity, before loading perovskites, approaches such as

heating, chemical treatment like acid-modification and metal-modification can be applied [70]. HCl can be used to modify the natural zeolite prior to the LFO loading. The acid treatment approach can remove amorphous impurities and provide zeolite with larger surface area and more available pore volume for easy incorporation of LFO. Loading 30% STO on HZSM-5 zeolite results in STO/HZSM-5 with high surface area, leading to high photocatalytic degradation rate towards Reactive Brilliant Red-X3B [71]. The HZSM-5 is capable of mediating electron migration and extending the lifetime of photogenerated charge carriers, thus leading to high photocatalytic activity towards organic pollutants.

3.3 Synthesis of various perovskite nanostructure

Constructing perovskite with various nanostructures can lead to full utilisation of solar energy, efficient light absorption and effective e^--h^+ separation. Perovskite with various structures such as nanoparticles with/without Hierarchical porous structure, core-shell structure, nanotubes, nanocubes and nanofilm have also been proven to offer significantly high photocatalytic response [72]. A well-designed nanoscale and hierarchically porous perovskite structure usually provides high surface area and excellent light absorption efficiency to take full advantage of reflection, refraction and scattering of photons [73]. A smaller size perovskite increases the availability of multiple reactive sites for enhanced photocatalytic reaction and higher degradation efficiency [74]. Downsizing perovskites to nanoscale with desired morphologies and functional properties holds a tremendous opportunity for obtaining excellent photo-catalysts as decreasing the particle size leads to an increase in the quantum yields of perovskite photocatalytic reactions [75]. In smaller size perovskite particles, shorter time is required for the photoinduced charge carriers to be diffused from the bulk to the surface of perovskite, thereby suppressing the recombination of the electrons and holes. Besides, the properties and the unique architecture that are achieved by down-sizing perovskites to nanoscale allow for direct use of visible light to remove pollut-ants without chemical addition. However, with decreasing the perovskite particle size to nanoscale the surface tension of perovskite nanoparticles significantly increases, which inevitably leads to particle aggregation.

In a bid to enhance the photocatalytic properties of perovskite with higher degradation efficiency of organic pollutants in water, a number of studies have been carried out to produce various novel nanoscale structures with unique properties [76–79]. The approaches that can be used to downsize perovskite particle and control its size are ball milling, ultrasonic treatment, micro emulsion method, addition of chelating agents and controlling the calcination temperature [80, 81]. A number of studies have used ball milling to downsize perovskite particle size. By controlling ball milling time duration, the particle size and defects of STO can be adjusted, for example, by increasing ball milling treatment time the particle size can be significantly decreased [82]. The smaller STO particles can provide shorter charge carriers transport path to the surface, where the photocatalytic reaction take place, thus decreasing the chance of photoinduced e^--h^+ pairs recombination. On the other hand, longer ball milling treatment time results in the creation of defects like oxygen vacancies, which act as a mediator and further facilitates the charge separation to accelerate the degradation of organic pollutant molecules. Nanoscale (15 nm aver-age thickness and 70–80 nm length) floral-like LFO 3D structure has been prepared via hydrothermal method using polyvinylpyrrolidone (PVP) as a chelating agent. Apparently, the photocatalytic activity of the nanoscale engineered LFO for the

degradation of organic pollutants is much higher than that of the bulk LFO, owing to the higher surface area (90.25 m^2/g as compared to bulk LFO of 8 m^2/g) that provides abundant active sites and efficient separation of e^--h^+ pairs via facile charge transport on small-sized nanosheets.

Over the last decade, several hierarchical nanostructure perovskites with different and effective morphology have been synthesised to enhance perovskite photocatalytic performance water decontamination [83, 84]. Hierarchical porous structure is one of the morphologies that provides larger surface area and more active sites, both of which enhance the contact between perovskite and organic pollutants during photocatalytic reaction [85]. Porous structure enhances the rate of mass transfer of pollutants within the perovskite, leading to an excellent photocatalytic activity with fast reaction kinetics for organic pollutant degradation. Porous nanofiber structure has also been synthesised for the enhancement of physical and chemical properties of perovskites compared to their granulate counterpart. Perovskite nanofiber structure can be synthesised using several approaches such as electrospinning method, template synthesis, hydrothermal method, self-assembly and solvothermal method, amongst which electrospinning method is widely regarded as a simple and easily controllable method for the fabrication of nanofibers [86]. The enhanced photocatalytic efficiency and higher removal of pollutants in water achieved by perovskite nanofiber structure can be attributed to the abundant and reachable active sites and the ultralong 1D nanostructure, both of which provide effective directing photogenerated electrons transportation [87, 88], as illustrated in **Figure 7**. The LaCoO$_3$ nanofiber structure has been shown to exhibit a higher photocatalytic activity than the LaCoO$_3$ nanoparticles in the degradation of RhB, owing to the favorable features of nanofiber structure such as larger surface area with more photoactive sites [23, 89]. The LFO ribbon-like porous ultrafine nanofibers have been synthesised by electrospinning, which exhibit higher specific surface area and more active sites for enhanced light absorption and photocatalytic degradation of MB.

The interfacial area of perovskite nanoparticles can be maximised by developing the Core-shell heterostructure with 3D hierarchical contact between the core and shell layers, in which a broader platform for charge carrier migration is provided. Various methods have been developed for synthesis of core-shell nanostructure
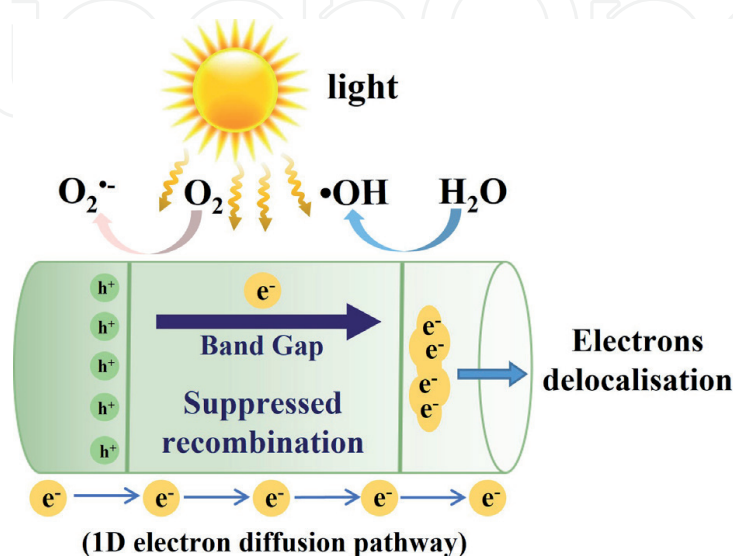
Figure 7.
Schematic representation of electron-hole pair separation in perovskite nanofiber systems.

perovskite such as surface functionalisation, template-sacrificial method and self-assembly method [90–92]. A heterostructure core-shell morphology enhances light absorption and multiple reflection of incident light, thus high light-harvesting efficiency, which makes core-shell perovskite structure ideal for photocatalytic applications, where charge separation is highly desirable [93]. A unique structure and heterojunction perovskite-based particles have been developed by coupling perovskites ($SrTiO_3$, $LaFeO_3$, $LaMnO_3$, $LaNiO_3$) with semiconductors (TiO_2, ZnO and SnO_2) as a core or shell to achieve an effective charge separation [94, 95]. LFO/TiO_2 core/shell heterostructure has been developed as photocatalysts with significantly improved photocatalytic activity for the degradation of myclobutanil pesticide under solar light and visible light irradiation [96]. The LFO shell acts as photosensitizer of TiO_2 for visible-light harvesting, and the full interphase contact between the core LFO and shell TiO_2 provides extensive charge transfer by driving electrons to the TiO_2 core and holes reversely to the LFO shell, which results in remarkably enhanced ·OH and $O_2^{\bullet-}$ generation for photodegradation of organic pollutants. A core-shell perovskite, $(Ba,Sr)TiO_3$ as core and TiO_2 as shell, has been reported to have an enhanced photocatalytic activity, due to charge separation efficiency across the core-shell interface.

Amongst the aforementioned nano structures, nanotube array has been widely studied for the enhancement of the photocatalytic activities of perovskites, due to their tunable size, uniformly aligned tubular structure, large internal surface area and fast electron transmission [97, 98].

4. Conclusions and future trends

Perovskites are highly crystalline and stable materials with unique and excellent features, which render them to be the best candidates amongst other semiconductor photocatalysts for photocatalytic degradation of organic pollutants. Their structure allows for tunning and adjusting their physiochemical properties through regulating their chemical composition, which offer a wide scope in developing novel nanocomposites.

Knowing that pristine perovskites suffer from a number of limitations such as low photocatalytic efficiency, insufficient solar energy consumption, rapid recombination of electron-hole and low redox potential, the great flexibility in regulating their physiochemical properties has been capitalised with the aim of developing perovskite-based materials with efficient photocatalytic activity in water remediation. A large number of perovskite-based nanocomposites have been developed and studied, using various synthesis methods and strategies such as partial and full cationic substitution using certain dopants, structure rescaling through downsizing and morphology alteration, coating and coupling with other advanced oxidation processes. Designing and preparing novel perovskite-based nanocomposites via these strategies, particularly partial and full cationic substitution, is elegant and can produce reasonably efficient photocatalysts, albeit it is still challenging.

Capitalising on the ability of computational tools, such as Density Functional Theory (DFT) based band structure, which are very effective for designing and understanding novel materials, will lead to further understanding of quantitative properties of these materials and shorten the selection process. Most of the perovskite-based nanocomposites exhibit promising photocatalytic performance, which can be considered as a viable solution to the problem of persistent organic pollutants faced by the living world and environment. However, a comprehensive study on these novel materials, particularly their ability in photocatalytic degradation

of a wide range of organic pollutants is limited. The majority of the developed perovskite-based nanocomposites have been tested on synthetic wastewater under laboratory conditions, which does not quite represent natural wastewater with organic pollutants. It is worth pointing out that in natural wastewater organic pollutants can affect photocatalytic efficiency through radical scavenging and attenuation of radiation in photocatalytic process. Using actual water and studying the perovskite-based materials provide more opportunities for large applications. Rescaling the structure of perovskite nanocomposites and alteration of their morphologies, for example creation of hierarchical pore structure, may be sufficient to enhance some aspects of photocatalytic activity in the degradation of a particular dye or pollutant. Further work on the relationship between the structure and physicochemical properties of these nanocomposites will be beneficial for further enhancement of photocatalytic activities of these materials and providing a novel insight over structure-property relation. Partial and full substitution strategy using different dopants is mainly used to promote light absorption, which in turn enhances the photocatalytic activity. A comprehensive knowledge on the effects of these dopants on the photophysical properties of the modified perovskite materials will further reveal the capabilities of perovskite-based nanocomposites and pave the way for future development perovskite-based photocatalysts with superior photocatalytic activity. The main focus of almost all the studies has been on the small production of small laboratory-scale materials, incorporating 3D printing and testing the produced materials will certainly be beneficial for large-scale synthesis, leading to industrial production. Membrane filtration is usually the main separation process that is used for separating the catalysts, however, using membrane to recover perovskite-based catalysts makes the water treatment process costly and quite complex, particularly due to the occurrence of membrane fouling. Therefore, recovery and recycling the perovskite-based nanocomposites after water decontamination process merit thorough investigations.

Acknowledgements

Author details

Yousef Faraj[1]* and Ruzhen Xie[2]

1 University of Chester, Chester, UK

2 Sichuan University, Chengdu, China

*Address all correspondence to: y.faraj@chester.ac.uk

IntechOpen

References

[1] Hejazi R, Mahjoub AR, Khavar AHC, Khazaee Z. Novel visible-light-responsive rGO-ZnO@Bi2MoO6 nanocomposite with enhanced light harvesting and Z-scheme charge transfer for photodegradation and detoxification of RhB. Solid State Sciences. 2019;**2019**:105934

[2] Robertson PKJ, Robertson JMC, Bahnemann DW. Removal of microorganisms and their chemical metabolites from water using semiconductor photocatalysis. Journal of Hazardous Materials. 2012;**211**:161-171

[3] Yao XX, Hu XL, Zhang WJ, Gong XY, Wang X, Pillai SC, et al. Mie resonance in hollow nanoshells of ternary TiO_2-Au-CdS and enhanced photocatalytic hydrogen evolution. Applied Catalysis B: Environmental. 2020;**276**:119153

[4] Devi LG, Kavitha R. A review on non metal ion doped titania for the photocatalytic degradation of organic pollutants under UV/solar light: Role of photogenerated charge carrier dynamics in enhancing the activity. Applied Catalysis B: Environmental. 2013;**140**:559-587

[5] Salas SE, Rosales BS, de Lase H. Quantum yield with platinum modified TiO_2 photocatalyst for hydrogen production. Applied Catalysis B: Environmental. 2013;**140**:523-536

[6] Loeb SK, Alvarez PJJ, Brame JA, Cates EL, Choi W, Crittenden J, et al. The technology horizon for photocatalytic water treatment: Sunrise or sunset? Environmental Science & Technology. 2019;**53**:2937-2947

[7] Shu LN, Sunarso J, Hashim SS, Mao JK, Zhou W, Liang FL. Advanced perovskite anodes for solid oxide fuel cells: A review. International Journal of Hydrogen Energy. 2019;**44**:31275-31304

[8] Garcia-Munoz P, Lefevre C, Robert D, Keller N. Ti-substituted $LaFeO_3$ perovskite as photoassisted CWPO catalyst for water treatment. Applied Catalysis B: Environmental. 2019;**248**:120-128

[9] Wang HL, Zhang LS, Chen ZG, Hu JQ, Li SJ, Wang ZH, et al. Semiconductor heterojunction photocatalysts: Design, construction, and photocatalytic performances. Chemical Society Reviews. 2014;**43**:5234-5244

[10] Sulaeman U, Yin S, Sato T. Visible light photocatalytic activity induced by the carboxyl group chemically bonded on the surface of $SrTiO_3$. Applied Catalysis B: Environmental. 2011;**102**:286-290

[11] Luo XS, Bai LM, Xing JJ, Zhu XW, Xu DL, Xie BH, et al. Ordered mesoporous cobalt containing perovskite as a high-performance heterogeneous catalyst in activation of peroxymonosulfate. ACS Applied Materials & Interfaces. 2019;**11**:35720-35728

[12] Sun J, Wei HZ, An LY, Jin CY, Wu HL, Xiong ZA, et al. Oxygen vacancy mediated La1-xCexFeO3-delta perovskite oxides as efficient catalysts for CWAO of acrylic acid by A-site Ce doping. Applied Catalysis B: Environmental. 2019;**245**:20-28

[13] Ye TN, Dong ZH, Zhao YN, Yu JG, Wang FQ, Guo SK, et al. Controllable fabrication of perovskite $SrZrO_3$ hollow cuboidal nanoshells. CrystEngComm. 2011;**13**:3842-3847

[14] Li XZ, Shi HY, Zhu W, Zuo SX, Lu XW, Luo SP, et al. Nanocomposite

LaFe1-xNixO$_3$/Palygorskite catalyst for photo-assisted reduction of NOx: Effect of Ni doping. Applied Catalysis B: Environmental. 2018;**23**:92-100

[15] He Z, Sun XY, Gu X. SrTiO$_3$ nanoparticles and nanofibers: Synthesis and comparison of photocatalytic properties. Journal of Material Science. 2017;**28**:13950-13955

[16] Karthikeyan C, Arunachalam P, Ramachandran K, Al-Mayouf AM, Karuppuchamy S. Recent advances in semiconductor metal oxides with enhanced methods for solar photocatalytic applications. Journal of Alloys and Compounds. 2020;**828**:154281

[17] Herrmann JM. Heterogeneous photocatalysis: Fundamentals and applications to the removal of various types of aqueous pollutants. Catalysis Today. 1999;**53**:115-129

[18] Wei K, Faraj Y, Yao G, Xie R, Lai B. Strategies for improving perovskite photocatalysts reactivity for organic pollutants degradation: A review on recent progress. Chemical Engineering Journal. 2021;**414**:128783

[19] Luo J, Li R, Chen YQ, Zhou XS, Ning XM, Zhan L, et al. Rational design of Z-scheme LaFeO3/SnS2 hybrid with boosted visible light photocatalytic activity towards tetracycline degradation. Separation and Purification Technology. 2019;**210**:417-430

[20] Jiang DL, Wang TY, Xu Q, Li D, Meng SC, Chen M. Perovskite oxide ultrathin nanosheets/g-C3N4 2D-2D heterojunction photocatalysts with significantly enhanced photocatalytic activity towards the photodegradation of tetracycline. Applied Catalysis B: Environmental. 2017;**201**:617-628

[21] Zhang Q, Huang Y, Peng SQ, Zhang YF, Shen ZX, Cao JJ, et al.

Perovskite LaFeO3-SrTiO$_3$ composite for synergistically enhanced NO removal under visible light excitation. Applied Catalysis B: Environmental. 2017;**204**:346-357

[22] Schneider J, Matsuoka M, Takeuchi M, Zhang JL, Horiuchi Y, Anpo M, et al. Understanding TiO$_2$ photocatalysis: Mechanisms and materials. Chemical Reviews. 2014;**114**:9919-9986

[23] Li Y, Gao XP, Li GR, Pan GL, Yan L, Zhu HY. Titanate nanofiber reactivity: Fabrication of MTiO$_3$ (M = Ca, Sr, and Ba) perovskite oxides. Journal of Physical Chemistry C. 2009;**113**:4386-4394

[24] Jamil HAATS. Nano sized Fe doped strontium titanate for photocatalytic degradation of dibutyl phthalate under visible light. Advanced Materials Letters. 2016;**6**:467-471

[25] Goldschmidt VM. Die Gesetze der Krystallochemie. Naturwissenschaften. 1926:477-485

[26] Ji QQ, Bi L, Zhang JT, Cao HJ, Zhao XS. The role of oxygen vacancies of ABO(3) perovskite oxides in the oxygen reduction reaction. Energy & Environmental Science. 2020;**13**:1408-1428

[27] Haruna A, Abdulkadir I, Idris SO. Photocatalytic activity and doping effects of BiFeO$_3$ nanoparticles in model organic dyes. Heliyon. 2020;**6**:e03237

[28] Wang M, Zhao TT, Dong XL, Li M, Wang HQ. Effects of Ce substitution at the A-site of LaNi0.5Fe0.5O$_3$ perovskite on the enhanced catalytic activity for dry reforming of methane. Applied Catalysis B: Environmental. 2018;**224**:214-221

[29] Xu JF, Liu J, Zhao Z, Xu CM, Zheng JX, Duan AJ, et al. Easy synthesis of three-dimensionally ordered macroporous La1-xKxCoO$_3$ catalysts

and their high activities for the catalytic combustion of soot. Journal of Catalysis. 2011;**282**:1-12

[30] Bradha M, Vijayaraghavan T, Suriyaraj SP, Selvakumar R, Ashok AM. Synthesis of photocatalytic La(1-x) A(x)TiO(3.5-delta) (A=Ba, Sr, Ca) nano perovskites and their application for photocatalytic oxidation of congo red dye in aqueous solution. Journal of Rare Earths. 2015;**33**:160-167

[31] Zheng JQ, Zhu YJ, Xu JS, LuQ B, Qi C, Chen F, et al. Microwave-assisted rapid synthesis and photocatalytic activity of mesoporous Nd-doped SrTiO$_3$ nanospheres and nanoplates. Materials Letters. 2013;**100**:62-65

[32] Hou L, Sun GF, Liu K, Li GFM. Preparation, characterization and investigation of catalytic activity of Li-doped LaFeO$_3$ nanoparticles. Journal of Sol-Gel Science and Technology. 2006;**40**:9-14

[33] Li FT, Liu Y, Liu RH, Sun ZM, Zhao DS, Kou CG. Preparation of Ca-doped LaFeO$_3$ nanopowders in a reverse microemulsion and their visible light photocatalytic activity. Materials Letters. 2010;**64**:223-225

[34] Wang Q, Liu ZQ, Liu DM, Liu GS, Yang M, Cui FY, et al. Ultrathin two-dimensional BiOBrxI1-x solid solution with rich oxygen vacancies for enhanced visible-light-driven photoactivity in environmental remediation. Applied Catalysis B: Environmental. 2018;**236**:222-232

[35] Hou LW, Zhang H, Dong LH, Zhang L, Duprez D, Royer S. A simple non-aqueous route to nano-perovskite mixed oxides with improved catalytic properties. Catalysis Today. 2017;**287**:30-36

[36] Sulaeman U, Yin S, Sato T. Solvothermal synthesis and photocatalytic properties of chromium-doped SrTiO3 nanoparticles. Applied Catalysis B: Environmental. 2011;**105**:206-210

[37] Wu GL, Li P, Xu DB, Luo BF, Hong YZ, Shi WD, et al. Hydrothermal synthesis and visible-light-driven photocatalytic degradation for tetracycline of Mn-doped SrTiO$_3$ nanocubes. Applied Surface Science. 2015;**333**:39-47

[38] Zhu HK, Fang MH, Huang ZH, Liu YG, Chen K, Guan M, et al. Novel chromium doped perovskites A(2) ZnTiO(6) (A= Pr, Gd): Synthesis crystal structure and photocatalytic activity under simulated solar light irradiation. Applied Surface Science. 2017;**393**:348-356

[39] Reunchan P, Umezawa N, Ouyang SX, Ye JH. Mechanism of photocatalytic activities in Cr-doped SrTiO3 under visible-light irradiation: An insight from hybrid density-functional calculations. Physical Chemistry Chemical Physics. 2012;**14**:1876-1880

[40] Peng Q, Shan B, Wen YW, Chen R. Enhanced charge transport of LaFeO$_3$ via transition metal (Mn, Co, Cu) doping for visible light photoelectrochemical water oxidation. International Journal of Hydrogen Energy. 2015;**40**:15423-15431

[41] Bantawala H, Shenoy US, Bhat DK. Vanadium-doped SrTiO$_3$ nanocubes: Insight into role of vanadium in improving the photocatalytic activity. Applied Surface Science. 2020;**513**:145858

[42] Wu SX, Ma Z, Qin YN, He F, Jia LS, Zhang YJ. XPS study of copper doping TiO$_2$ photocatalyst. Acta Physico-Chimica Sinica. 2003;**19**:967-969

[43] Phan TTN, Nikoloski AN, Bahri PA, Li D. Heterogeneous photo-Fenton

degradation of organics using highly efficient Cu-doped LaFeO$_3$ under visible light. Journal of Industrial and Engineering Chemistry. 2018;**61**:53-64

[44] Peng JL, Lu XH, Jiang X, Zhang YH, Chen QX, Lai B, et al. Degradation of atrazine by persulfate activation with copper sulfide (CuS): Kinetics study, degradation pathways and mechanism. Chemical Engineering Journal. 2018;**354**:740-752

[45] Wei ZX, Wang Y, Liu JP, Xiao CM, Zeng WW. Synthesis, magnetization and photocatalytic activity of LaFeO$_3$ and LaFe0.5Mn0.5−xO3−δ. Materials Chemistry and Physics. 2012;**136**:755-761

[46] Hoang VQT, Phan TQP, Senthilkumar V, Doan VT, Kim YS, Le MV. Enhanced photocatalytic activities of vandium and molybdenum co-doped strontium titanate under visible light. International Journal of Applied Ceramic Technology. 2019;**16**:1651-1658

[47] Kato H, Kudo A. Visible-light-response and photocatalytic activities of TiO2 and SrTiO$_3$ photocatalysts codoped with antimony and chromium. The Journal of Physical Chemistry. B. 2002;**106**:5029-5034

[48] Jamil TS, Abbas HA, Youssief AM, Mansor ES, Hammad FF. The synthesis of nano-sized undoped, Bi doped and Bi, Cu co-doped SrTiO$_3$ using two solegel methods to enhance the photocatalytic performance for the degradation of dibutyl phthalate under visible light. Comptes Rendus Chimie. 2017;**20**:97-106

[49] Li F, Yu K, Lou LL, Su ZQ, Liu SX. Theoretical and experimental study of La/Ni co-doped SrTiO3 photocatalyst. Material Science Engineering B Advanced. 2010;**172**:136-141

[50] Zou F, Jiang Z, Qin XQ, Zhao YX, Jiang LY, Zhi JF, et al. Template-free synthesis of mesoporous N-doped SrTiO3 perovskite with high visible-light-driven photocatalytic activity. Chemical Communications. 2012;**48**:8514-8516

[51] Khazaee Z, Mahjoub AR, Khavar AHC, Srivastava V, Sillanpaa M. Synthesis of layered perovskite Ag,F-Bi2MoO6/rGO: A surface plasmon resonance and oxygen vacancy promoted nanocomposite as a visible-light photocatalyst. Journal of Photochemistry and Photobiology A. 2019;**379**:130-143

[52] Hu J, Ma JH, Wang L, Huang H, Ma LW. Preparation, characterization and photocatalytic activity of Co-doped LaMnO$_3$/graphene composites. Powder Technology. 2014;**254**:556-562

[53] Chang CW, Hu CC. Graphene oxide-derived carbon-doped SrTiO$_3$ for highly efficient photocatalytic degradation of organic pollutants under visible light irradiation. Chemical Engineering Journal. 2020;**383**:123116

[54] Wu Y, Wang H, Tu W, Liu Y, Tan YZ, Yuan XZ, et al. Quasi-polymeric construction of stable perovskite-type LaFeO3/g-C3N4 heterostructured photocatalyst for improved Z-scheme photocatalytic activity via solid p-n heterojunction interfacial effect. Journal of Hazardous Materials. 2018;**347**:412-422

[55] Nousir S, Keav S, Barbier-Jr J, Bensitel M, Brahmi R, Duprez D. Deactivation phenomena during catalytic wet air oxidation (CWAO) of phenol over platinum catalysts supported on ceria and ceria-zirconia mixed oxides. Applied Catalysis B: Environmental. 2008;**84**:723-731

[56] Jian D, Gao PX, Cai WJ, Allimi BS, Alpay SP, Ding Y, et al. Synthesis,

characterization, and photocatalytic properties of ZnO/(La,Sr)CoO3 composite nanorod arrays. Journal of Materials Chemistry. 2009;**19**:970-975

[57] Song S, Xu LJ, He ZQ, Chen JM, Xiao XZ, Yan B. Mechanism of the photocatalytic degradation of CI reactive black 5 at pH 12.0 using SrTiO3/CeO$_2$ as the catalyst. Environmental Science & Technology. 2007;**41**:5846-5853

[58] Zhang RJ, Wan YJ, Peng JL, Yao G, Zhang YH, Lai B. Efficient degradation of atrazine by LaCoO$_3$/Al$_2$O$_3$ catalyzed peroxymonosulfate: Performance, degradation intermediates and mechanism. Chemical Engineering Journal. 2019;**372**:796-808

[59] Yang JS, Li LM, Yang XS, Song S, Li J, Jing FL, et al. Enhanced catalytic performances of in situ-assembled LaMnO$_3$/delta-MnO$_2$ hetero-structures for toluene combustion. Catalysis Today. 2019;**327**:19-27

[60] Gong C, Zhang ZY, Lin S, Wu Z, Sun L, Ye CQ, et al. Electrochemical synthesis of perovskite LaFeO$_3$ nanoparticle-modified TiO$_2$ nanotube arrays for enhanced visible-light photocatalytic activity. New Journal of Chemistry. 2019;**43**:16506-16514

[61] Kumar RD, Thangappan R, Jayavel R. Synthesis and characterization of LaFeO$_3$/TiO$_2$ nanocomposites for visible light photocatalytic activity. Journal of Physics and Chemistry of Solids. 2017;**101**:25-33

[62] Chen C, Zhou JL, Geng JF, Bao RY, Wang ZH, Xia JX, et al. Perovskite LaNiO$_3$/TiO$_2$ step-scheme heterojunction with enhanced photocatalytic activity. Applied Surface Science. 2020;**503**:144287

[63] Cao TP, Li YJ, Wang CH, Shao CL, Liu YC. A facile in situ hydrothermal method to SrTiO$_3$/TiO$_2$ nanofiber heterostructures with high photocatalytic Aactivity. Langmuir. 2011;**27**:2946-2952

[64] Liu X, Jiang JZ, Jia YS, Qiu JM, Xia TL, Zhang YH, et al. Insight into synergistically enhanced adsorption and visible light photocatalytic performance of Z-scheme heterojunction of SrTiO$_3$(La,Cr)-decorated WO$_3$ nanosheets. Applied Surface Science. 2017;**412**:279-289

[65] Phan TTN, Nikoloski AN, Bahri PA, Li D. Adsorption and photo-Fenton catalytic degradation of organic dyes over crystalline LaFeO$_3$-doped porous silica. RSC Advances. 2018;**8**:36181-36190

[66] Cao X, Luo SQ, Liu C, Chen JW. Synthesis of bentonite-supported Fe$_2$O$_3$-doped TiO$_2$ superstructures for highly promoted photocatalytic activity and recyclability. Advanced Powder Technology. 2017;**28**:993-999

[67] Phan TTN, Nikoloski AN, Bahri PA, Li D. Facile fabrication of perovskite-incorporated hierarchically mesoporous/macroporous silica for efficient photoassisted-Fenton degradation of dye. Applied Surface Science. 2019;**491**:488-496

[68] Li HL, Zhu JJ, Xiao P, Zhan YY, Lv KL, Wu LY, et al. On the mechanism of oxidative degradation of rhodamine B over LaFeO$_3$ catalysts supported on silica materials: Role of support. Microporous and Mesoporous Materials. 2016;**221**:159-166

[69] Li HL, Zhang WJ, Liu YX. HZSM-5 zeolite supported boron-doped TiO$_2$ for photocatalytic degradation of ofloxacin. Journal of Materials Research and Technology. 2020;**9**:2557-2567

[70] Wang XY, Ozdemir O, Hampton MA, Nguyen AV, Do DD. The effect of zeolite

treatment by acids on sodium adsorption ratio of coal seam gas water. Water Research. 2012;**46**:5247-5254

[71] Zhang WJ, Du L, Bi FF, He HB. A novel SrTiO3/HZSM-5 photocatalyst prepared by sol-gel method. Materials Letters. 2015;**157**:103-105

[72] Qin CX, Li ZY, Chen GQ, Zhao Y, Lin T. Fabrication and visible-light photocatalytic behavior of perovskite praseodymium ferrite porous nanotubes. Journal of Power Sources. 2015;**285**:178-184

[73] Faisal M, Harraz FA, Ismail A, El-Toni AM, Al-Sayari SA, Al-Hajry A, et al. Polythiophene/mesoporous SrTiO$_3$ nanocomposites with enhanced photocatalytic activity under visible light. Separation and Purification Technology. 2018;**190**:33-34

[74] Huo YS, Yang H, Xian T, Jiang JL, Wei ZQ, Li S, et al. A polyacrylamide gel route to different-sized CaTiO$_3$ nanoparticles and their photocatalytic activity for dye degradation. Journal of Sol-Gel Science and Technology. 2014;**71**:254-259

[75] Souza AE, Santos GTA, Barra BC, Macedo WD, Teixeira SR, Santos CM, et al. Photoluminescence of SrTiO$_3$: Influence of particle size and morphology. Crystal Growth & Design. 2012;**12**:5671-5679

[76] Thirumalairajan S, Girija K, Mastelaro VR, Ponpandian N. Photocatalytic degradation of organic dyes under visible light irradiation by floral-like LaFeO$_3$ nanostructures comprised of nanosheet petals. New Journal of Chemistry. 2014;**38**:5480-5490

[77] Su HJ, Jing LQ, Shi KY, Yao CH, Fu HG. Synthesis of large surface area LaFeO$_3$ nanoparticles by SBA-16

template method as high active visible photocatalysts. Journal of Nanoparticle Research. 2010;**12**:967-974

[78] Li SD, He ZX, Wang XL, Gao K. Fabrication of unique ribbon-like porous LaFeO3 nanofibers photocatalyst via electrospinning. Applied Physics A Materials. 2014;**117**:1381-1386

[79] Li L, Rohrer GS, Salvador PA. Heterostructured ceramic powders for photocatalytic hydrogen production: Nanostructured TiO$_2$ shells surrounding microcrystalline (Ba,Sr)TiO$_3$ cores. Journal of the American Ceramic Society. 2012;**95**:1414-1420

[80] Buscaglia V, Randall CA. Size and scaling effects in barium titanate. An overview. Journal of European Ceramic Society. 2020;**40**:3744-3758

[81] Singh H, Rajput JK. Novel perovskite nanocatalyst (BiFeO3) for the photodegradation of rhodamine B/tartrazine and swift reduction of nitro compounds. Journal of the Iranian Chemical Society. 2019;**16**:2409-2432

[82] Kumar V, Choudhary S, Malik V, Nagarajan R, Kandasami A, Subramanian A. Enhancement in photocatalytic activity of SrTiO$_3$ by tailoring particle size and defects. Physica Status Solidi A: Applications and Materials Science. 2019;**216**:1900294

[83] Humayun M, Qu Y, Raziq F, Yan R, Li Z, Zhang X, et al. Exceptional visible-light activities of TiO$_2$-coupled N-doped porous perovskite LaFeO$_3$ for 2,4-dichlorophenol decomposition and CO$_2$ conversion. Environmental Science & Technology. 2016;**50**:13600-13610

[84] Cruz del Álamo A, González C, Pariente MI, Molina R, Martínez F. Fenton-like catalyst based on a reticulated porous perovskite

material: Activity and stability for the on-site removal of pharmaceutical micropollutans in a hospital wastewater. Chemical English Journal. 2020;**401**:126113

[85] Afzal S, Quan X, Zhang JL. High surface area mesoporous nanocast LaMO3 (M = Mn, Fe) perovskites for efficient catalytic ozonation and an insight into probable catalytic mechanism. Applied Catalysis B: Environmental. 2017;**206**:692-703

[86] Dong B, Li ZC, Li ZY, Xu XR, Song MX, Zheng W, et al. Highly efficient LaCoO$_3$ nanofibers catalysts for photocatalytic degradation of Rhodamine B. Journal of the American Ceramic Society. 2010;**93**:3587-3590

[87] Yun HJ, Lee H, Joo JB, Kim W, Yi J. Influence of aspect ratio of TiO$_2$ nanorods on the photocatalytic decomposition of formic acid. Journal of Physical Chemistry C. 2009;**113**:3050-3055

[88] Liu Y, Zhang MY, Li L, Zhang XT. One-dimensional visible-light-driven bifunctional photocatalysts based on Bi4Ti3O12 nanofiber frameworks and Bi2XO6 (X = Mo, W) nanosheets. Applied Catalysis B: Environmental. 2014;**160**:757-766

[89] Zhu K, Vinzant TB, Neale NR, Frank AJ. Removing structural disorder from oriented TiO$_2$ nanotube arrays: Reducing the dimensionality of transport and recombination in dye-sensitized solar cells. Nano Letters. 2007;**7**:3739-3746

[90] Pan CS, Xu J, Wang YJ, Li D, Zhu YF. Dramatic activity of C$_3$N$_4$/BiPO$_4$ photocatalyst with core/shell structure formed by self-assembly. Advanced Functional Materials. 2012;**22**:1518-1524

[91] Kumar S, Khanchandani S, Thirumal M, Ganguli AK. Achieving enhanced visible-light-driven photocatalysis using Type-II NaNbO$_3$/CdS core/shell heterostructures. ACS Applied Materials & Interfaces. 2014;**6**:13221-13233

[92] Wei YZ, Wang JY, Yu RB, Wan JW, Wang D. Constructing SrTiO$_3$-TiO$_2$ heterogeneous hollow multi-shelled structures for enhanced solar water splitting. Angewandte Chemie International. 2019;**58**:1422-1426

[93] Zhang N, Xu YJ. Aggregation- and leaching-resistant, reusable, and multifunctional Pd@CeO$_2$ as a robust nanocatalyst achieved by a hollow core-shell strategy. Chemistry of Materials. 2013;**25**:1979-1988

[94] Wang SB, Ren Z, Song WQ, Guo YB, Zhang MW, Suib SL, et al. ZnO/perovskite core-shell nanorod array based monolithic catalysts with enhanced propane oxidation and material utilization efficiency at low temperature. Catalysis Today. 2015;**258**:549-555

[95] Do JY, Im Y, Kwak BS, Park SM, Kang M. Preparation of basalt fiber@perovskite PbTiO$_3$ core-shell composites and their effects on CH$_4$ production from CO$_2$ photoreduction. Ceramics International. 2016;**42**:5942-5951

[96] Garcia-Munoz P, Fresno F, Ivanez J, Robert D, Keller N. Activity enhancement pathways in LaFeO$_3$@TiO$_2$ heterojunction photocatalysts for visible and solar light driven degradation of myclobutanil pesticide in water. Journal of Hazardous Materials. 2020;**400**:123099

[97] Chen X, He XF, Yang X, Wu ZS, Li YF. Construction of novel 2D/1D g-C3N4/CaTiO3 heterojunction with face-to-face contact for boosting

photodegradation of triphenylmethane dyes under simulated sunlight. Journal of Taiwan Institute of Chemical Engineers. 2020;**107**:98-109

[98] Deng AJ, Chen JF, Li HL, Ren JL, Sun R, Zhao LH. Photo-degradation of methyl orange by polysaccharides/LaFe$_{0.8}$Cu$_{0.2}$O$_3$ composite films. BioResources. 2014;**9**:2717-2726

[99] Dhiman M, Singhal S. Effect of doping of different rare earth (europium, gadolinium, dysprosium and neodymium) metal ions on structural, optical and photocatalytic properties of LaFeO$_3$ perovskites. Journal of Rare Earths. 2019;**37**:1279-1287

[100] Humayun M, Raziq F, Zhang XL, Yan R, Li ZJ, Qu Y, et al. Synthesis of ZnO/Bi-doped porous LaFeO$_3$ nanocomposites as highly efficient nano-photocatalysts dependent on the enhanced utilization of visible-light-excited electrons. Applied Catalysis B: Environmental. 2018;**231**:23-33

[101] Fu XX, Yang QH, Sang LX. Studies on photocatalytic activity of perovskite type LaFe1-xCuxO$_3$. Chemical Journal of Chinese Universities Chinese. 2002;**23**:283-286

[102] Tonda S, Kumar S, Anjaneyulu O, Shanker V. Synthesis of Cr and La-codoped SrTiO$_3$ nanoparticles for enhanced photocatalytic performance under sunlight irradiation. Physical Chemistry Chemical Physics. 2014;**16**:23819-23828

[103] Ha MN, Chao ZL, Zhao Z. Doping effects on mixed-phase crystalline perovskite AxSr1−xFeO3−δ (A = Pr, Sm; $0 \leq x \leq 0.8$) nanoparticles and their application for photodegradation of rhodamine B. Research on Chemical Intermediates. 2018;**45**:1493-1508

[104] Abdi M, Mahdikhah V, Sheibani S. Visible light photocatalytic

performance of La-Fe co-doped SrTiO$_3$ perovskite powder. Optical Materials. 2020;**102**:109803

[105] Wang Y, Ma W, Song Y, et al. Enhanced photocatalytic performance of SrTiO$_3$ powder induced by Eu dopants. Journal of Rare Earths. 2020;**39**:541-547